International Conference on Renewable Energies and Power Quality (ICREPQ'13)
Bilbao (Spain), 20th to 22th March, 2013
Renewable Energy and Power Quality Journal (RE&PQJ)
ISSN 2172-038 X, No.11, April 2013

Back-pass non-perforated unglazed solar collector: performance and evaluation

M A Paya-Marin[1], J B P Lim[1], B Sen Gupta[1] and R M Lawson[2]

[1] School of Planning, Architecture and Civil Engineering Queen's University Belfast
SPACE, David Keir Building, Belfast, BT9 5AG (U.K.)
Phone/Fax number +44 (0)28 9097 5456, e-mail: **mpaya01@qub.ac.uk**, **j.lim@qub.ac.uk**, **b.sengupta@qub.ac.uk**

[2] Faculty of Engineering and Physical Sciences, University of Surrey
Guildford, Surrey, GU2 7XH (U.K.)
Phone/Fax number +44 (0)1483 686617, e-mail: **m.lawson@surrey.ac.uk**

Abstract.

The thermal efficiency is investigated of the new Kingspan back pass non-perforated unglazed solar collector (BPSC). This technology incorporated into the building sector, can potentially change the role of the building envelope from passive energy conservation, to that of producer of energy. BPSC can be used as a preheated air source for heating and ventilation, leading to a reduction in energy consumption. The BPSC system can potentially reduce the heating and monetary requirement for the buildings by 23%. Over a one year period, temperature rise at different heights, flow rates and solar radiations have been monitored. An equation to predict the temperature rise through the solar collector is proposed.

Key words

Thermal efficiency, back pass non-perforated unglazed solar collector, preheated air, solar air heaters.

1. Introduction

The operational energy of buildings account for 40% of the European Union's energy consumption and carbon emissions. Of this operational energy, approximately 50% is due to heating, ventilation and air conditioning services (HVAC) [1], of which only 1.8% in the UK is produced by renewable sources. The UK target for carbon emissions is to achieve an 80% reduction by 2050 [2].

A major challenge of the construction industry is to develop more efficient renewable energy technologies. One such technology is solar air collectors (SAC). These are cost-effective applications for new commercial buildings and industrial façades (Fig. 1). If developed and successfully incorporated into the building sector, such technologies can potentially change the role of the building envelope from one where the objective is passive energy conservation, to that of producer of energy [3].

SACs were first used in 1980 and since then have mainly been developed in North America [4].

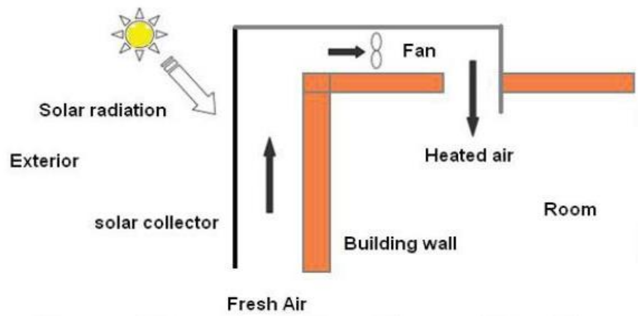

Fig. 1. Solar air collector system schematic

The first SAC system in the UK was installed in 2006. Its performance was monitored during its first year and it was found that the heat generated by the SAC was 79,191 kWh, representing 21% of the heating demand of the previous year. Since its introduction, the use of SACs in the UK has been increasing. [1]

This paper describes the new Kingspan back pass non-perforated solar collectors (BPSC) Fig. 2.

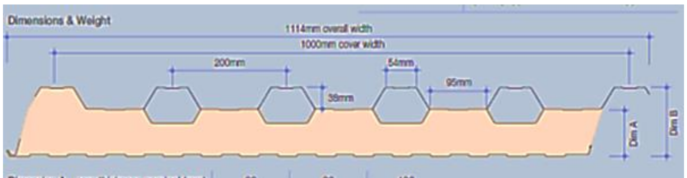

Dimension A - core thickness nominal (mm)	68	80	100
Dimension B - overall dimension (mm)	106	118	138
Weight kg/m²	11.5	12.0	12.8

Fig. 2. BPSC cross section and measures

BPSCs can be used as a preheated air source for heating and ventilation, leading to a reduction in energy consumption. Details of the BPSC are shown in Fig. 3. As can be seen, by utilizing the outer steel skin of the panel as a solar collector, the incident solar radiation is absorbed, causing a rapid temperature rise. The magnitude of the temperature rise is dependent on the intensity of the solar radiation, the air flow rate through the collector crowns and the solar collector height. Kingspan modified an existing five crowns composite panel to create a BPSC where the fresh air is taken from the base of the profiled voids beneath the crowns of the panel (Fig. 4).

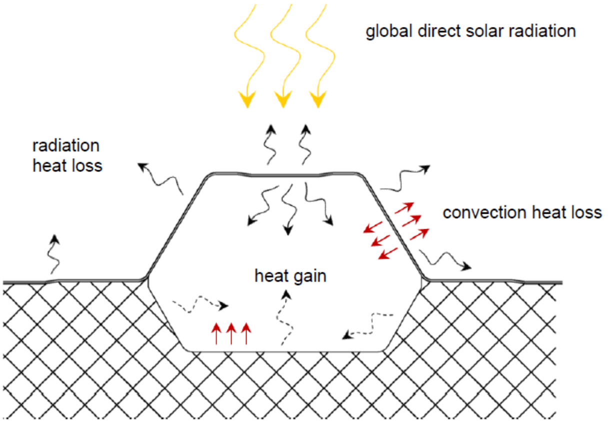

Fig.3. BPSC energy flow section.

No previous studies have been undertaken to assess the thermal performance and efficiencies of BPSC. The purpose of this paper is to analyse the BPSC to demonstrate the accuracy of the thermal theory, evaluate the efficiency of the key factors, and optimize them in order to provide an equation that can predict the temperature rise in different environments and situations.

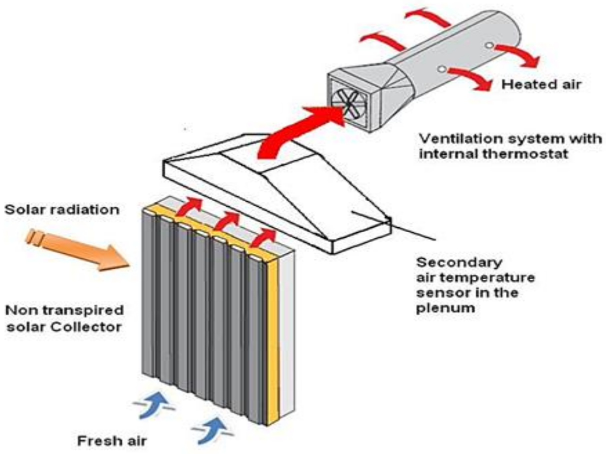

Fig.4. BPSC system schematic

2. Monitoring of performance of BPSC

Two identical buildings were erected at the Kingspan R&D centre to demonstrate the capability of BPSC's as a supplementary heating system (Fig. 5).
Both buildings were fitted with 12kW gas fired heaters and air-con units to ensure that the internal building environment is maintained constantly within the temperature range of 15-19°C. One test house had the SAC system installed whilst the other house acts as the control building. The exact heating requirements for the two test house buildings were continuously monitored and cumulatively recorded. For the given test building specification, the SAC system reduced the heating and monetary requirement for the test building by 23%.

Fig. 5 General view the two experimental buildings

3. Basic theory

The temperature rise of the air in the collector varies with the distance (height) from the air inlet. It approaches a "saturation temperature rise" (above ambient temperature and for an infinitely high collector or zero flow rate) asymptotically following an exponential approach curve. The saturation temperature rise depends on the absorptivity of the collector, the heat transfer coefficient between the collector surface and the environment (and hence on local windspeed), the heat transfer coefficient between the collector surface and the air in the collector (and thus potentially on flow rate), and the "back losses" from the collector to the environment behind it (usually the building interior) The exponential term also depends on the flow rate.

The quantity of heat delivered by the BPSC is given by equation 1 [5]:

$$\boldsymbol{Q} = \boldsymbol{m_{air}} \boldsymbol{C_p} \left(\boldsymbol{t_{out}} \text{-} \boldsymbol{t_{in}}\right) \qquad (1)$$

Where $\boldsymbol{C_p}$ is the specific heat air capacity (Kj/Kg C°), $\boldsymbol{m_{air}}$ is the mass flow rate though the BPSC (Kg/s), $\boldsymbol{t_{out}}$ is the dry bulb air temperature (C°), $\boldsymbol{t_{in}}$ is the inlet air temperature (C°).

The BPSC efficiency is given by equation 2 [5]

$$\boldsymbol{\mu} = \frac{\boldsymbol{Q}}{\boldsymbol{AG_{tot}}} \qquad (2)$$

Q is the heat output from the collector, given by the equation above. A is the gross useful area of the collector (m²), and G_{tot} is the total irradiance on the collector surface W/m²).

The total solar radiation is given by equation 3 [5]:

$$\boldsymbol{G_{tot=G}}_{\ \boldsymbol{solar}} \pm (\boldsymbol{\varepsilon}/\boldsymbol{\alpha})(\boldsymbol{E_L}\ \text{-}\boldsymbol{\sigma t_{amb}}^{\boldsymbol{4}}) \qquad (3)$$

Where σ is the Stefan-Boltzmann constant and is equal to 5.67 x 10^{-8} W/m² x K^4. ε is the remittance of the collector surface. α is the solar absorptance of the collector surface, E_L is the incident longwave radiation.

4. Rig test

A test rig was constructed at Kingspan research and development centre in Ireland, to determinate the BPSC efficiency and which are the main facts in the collector performance, (Fig.6). The 7.04m x 4m BPSC installed and linked to a rear plenum was connected to a fan inlet through a HVAC duct. An orifice plate was installed to take air flow rate measurements.

Five temperature sensors (PT 100) have been placed near the inlet channels at the bottom of the panel. The sensors were shielded in order to minimise radiation heat gain, such could give artificial readings. A humidity sensor (Rotronic hygrometer HC2-5) has been installed to measure the humidity of the internal airflow, the exact location is in the connection between the plenum and the duct. Five temperature sensors (PT 100) have been installed inside the duct, in the connection with the plenum; these sensors provide the measurements of the Dry bulb temperature. The duct overall is under slight negative pressure. The pressure upstream and downstream of the orifice plate is measured by two small holes in the duct and inserting the end of the pressure transmitter

A Pyrgeometer CGR4 and 2 CMP11 Pyrometer radiation sensors have been mounted in a vertical orientation.

Two anemometers (2 A 100L2) have been mounted in the same plane as the BPSC such that the wind speed across the surface is measured rather than the free-air, unobstructed wind speed.

Fig. 6 Rear view of the BPSC test rig

5. BPSC Calculations.

The orifice plate connected to the rig cover a maximum air flow rate of 2200m³/hr and the diameter of the orifice is 172.62mm. The duct diameter is 250mm.The total panel area is 7.040x4=28.16m² and the panel area below the plenum chamber is 6.5x4=26m². The active area of the panel is 0.583x4x6.5=15.16m³/m²; the flow rate targeted is 90 m³/hr. The total Flow rate for active panel area is 15.16x90=1364.4m³/hr/m² or 387.89 l/s.

Flow rate is given by equation 4 [7]:

$$q_m = \alpha\varepsilon\pi\frac{d^2}{4}\sqrt{2\rho_u\ \Delta_p} \qquad (4)$$

Where Flow rate coefficient is given by equation 5 [8]:

$$\propto = (1-\beta^4)^{-0,5}[0,5959+0,0312\beta^{2,1}-0,184\beta^8+0,0029\beta^{2,5}((\tfrac{10^6}{Re_D})^{0,75}] \qquad (5)$$

Reynolds number is given by equation 6 [8]:

$$R_D = \frac{\alpha\varepsilon\beta d}{v}\sqrt{\frac{2\Delta p}{\rho u}} \qquad (6)$$

Expansibility factor is given by equation 7 [8]:

$$\varepsilon = 1-(0,41+0,35\beta^4)\frac{\Delta p}{kp_u} \qquad (7)$$

Kinematic viscosity is given by equation 8 [8]:

$$v = \frac{(17,1+0,0048t_{out})^{-6}}{\rho u} \qquad (8)$$

Saturated vapour factor given by equation 9 [9]:

$$10^{(30,590521-8,2\log(\theta+273,15)+0,0024804(\theta+273,15)-(\frac{3142,31}{\theta+273,15}))} \qquad (9)$$

Enhanced factor given by equation 10 [10]:

$$f = 1 + A + P_a[\mathrm{B}+\mathrm{C}\ (t_{out} + \mathrm{D} + \mathrm{EP})^2] \qquad (10)$$

Partial vapour pressure given by equation 11 [9]:

$$P_v = (\frac{R_H}{100})\rho_s \qquad (11)$$

Molar ratio given by equation 12 [10]:

$$\propto_i = \frac{P_v}{P_a} \qquad (12)$$

Molar mass moist air given by equation 13 [10]:

$$\propto_a = \left(\frac{P_v}{P_a}\mu_{wat}\right) + (1-\frac{P_v}{P_a})\ \mu_{air} \qquad (13)$$

Equivalent gas constant given by equation 14 [10]:

$$R = \frac{\bar{R}}{\propto_a} \qquad (14)$$

Density at moist air given by equation 15 [10]:

$$\rho_u = \frac{P_a}{R(t_{out}+273,15)} \qquad (15)$$

The readings are taken every 5 seconds. In each test the following variables are achieved within the specified tolerance for a period of 25 minutes.

Parameter	**Symbol**	**Deviation from the mean value**
Total short wave solar irradiance	G_{tot}	± 50 W/m²
Long wave thermal irradiance	E_L	± 20 W/m²
Surrounding air temperature	t_{amb}	± 1K°
Fluid (air) mass flow rate	m_{air}	± 1%
Collector fluid inlet temperature	t_{in}	±0.1K°
Surrounding air speed	u	±0.5 m/s

Table1. Limits reproduced from EN 12975-2:2006 Table

The 25 min period actually constitutes a 15 min pre-conditioning period where the conditions should be stable, but is not used in the calculations, immediately followed by a 10 min measurement period from which the measurements are used to calculate the performance for given condition.

6. Experimental data

Data from 26 tests, of 25 minutes duration taken over one year period, have been analysed. A feature of the test results is the variation in energy collection under similar conditions. The following findings are based on results from individual tests of the particular configuration of collector tested.

6.1. Temperature rise and radiation

The tests were carried out at flow rates between 75 and 92m³/hr/m². For these conditions there is a fairly consistent trend of larger temperature rises at higher radiation levels.

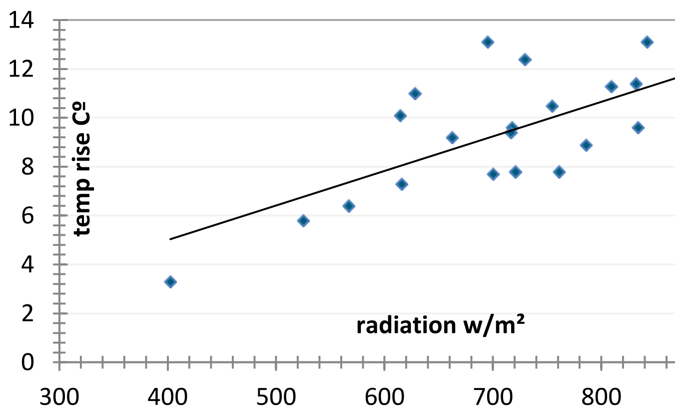

Fig.7 Variation of temperature rise against radiation for middle air flow rates.

6.2. Saturation temperature rise

The results for temperature rise per unit radiation show very little variation with flow rate, suggesting that the combination of flow rate and height is sufficient for the observed temperature increases to be close to saturation value. Fig. 7 shows the best estimate is 0.0143 deg C per W/m² with a standard deviation of 0.0028

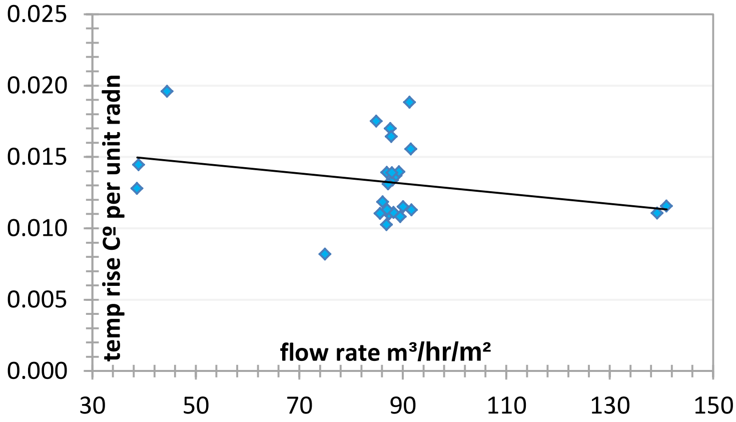

Fig.8 Variation of temperature rise per unit radiation against flow rates.

6.3. Characteristic height and sensitivity to collector height

According to the basic theory, the exponential parameter is characterised by the ratio between height and flow rate, which can be described as a characteristic length. The value of this parameter should theoretically vary linearly with flow rate. It can be estimated from the data collected by the tests. Within the scatter of the results linearity seems to be the case.

This relationship can be used to estimate the exit air temperature as a function of flow rate and height (and radiation level) and thus to estimate how the performance of the collector would vary with height. Qualitatively, if the collector height is large compared to the characteristic length the exit temperature will be close to the saturation temperature: if the height is small the exit temperature will be lower (but the efficiency will be higher).

The highest efficiencies are obtained with high flow rates and low-height collectors (Fig.9). For a given total air flow (defined by the room ventilation needs), splitting the flow between a series of low collectors has two effects: the low collector is inherently more efficient but this is exactly counterbalanced by the reduced flow rate per collector.

The best efficiency is obtained with high flow rates: however, if total collector area is not a constraint, maximum heat collection may be obtained by a larger area of lower flow (and therefore less efficient) collector. (The efficiency penalty for low flow is relatively small except at low flow rates)

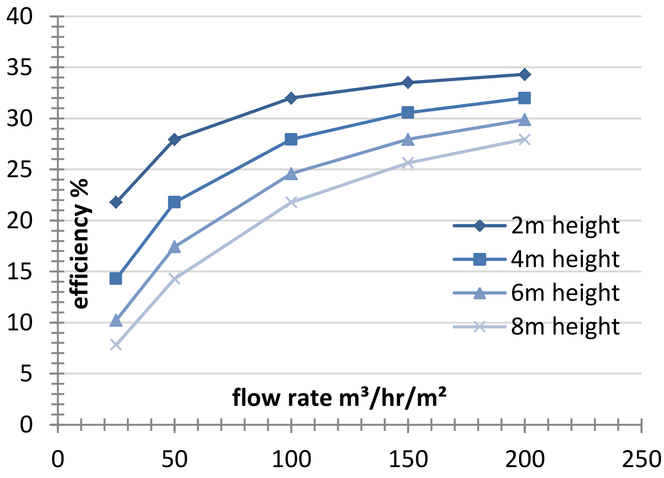

Fig.9 Variation of percentage efficiency against flow rate

6.4. Specific fan power

An approximate estimate can be made by using the CIBSE Guide C [9] pressure drop table for circular ductwork. At a velocity of 8 m/s a 50mm diameter duct has pressure drop of 24 Pa/m so a 6.5 m high collector would have a pressure drop of about 156 Pa (excluding additional losses due to bends etc.) and so, for an ideal fan, the specific fan power (SFP) will be increased by 0.156. For a typical fan, the increase will be about 0.3. The longer the duct length (that is the higher the collector) the larger the effect. Pressure drop is very sensitive to flow velocity so having the flow rate to 4 m/s reduces the pressure drop to about 4 Pa.
For a volume flow of 390 l/s, an increase of SFP of 0.3 equates to an electricity consumption of about 130 W. Building Regulations in the UK are based on carbon emissions. In carbon terms 130 W electricity is equivalent to 300 W of heat from a gas boiler. In addition, the ventilation system will presumably be drawing air through the collector whenever it is in operation, including periods of low solar radiation.

7. Discussion

The result shows that the temperature increases with the height/flow ratio up to certain point and is constant then, the collector height appears effectively infinite. ΔTs can be estimated from these values by using the data point from the highest value of the height/flow ratio: in this case 0.0143 (at a ratio of 0.223). Re-arranging the basic theory, the following equation is proposed:

$$\boldsymbol{Ln}\left(\frac{\Delta T}{\Delta Ts}\right) = \boldsymbol{E}(\boldsymbol{h}/\boldsymbol{q}) \qquad (16)$$

The estimation of E is -8.07/0.223=-36.19, giving a curve fit as show in the Fig.10. This illustrates that beyond a certain height to flow ratio, there is no additional heat collection.

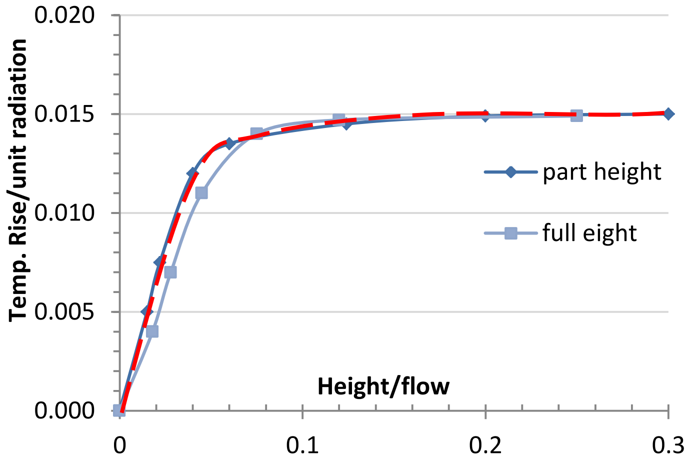

Fig.10 Variation of temperature rise per unit radiation against flow rates

8. Conclusion

It is found that Back-pass non-transpired solar collectors (BPSC) can provide a substantial energy savings in the form of pre-heated ventilation air. Temperature increases across the BPSC have been measured. The heat transfer theory and experimental analysis of the BPSC has shown that highest efficiencies can be achieved with a combination of collector highs and effective air flow rates.
Future work in this study will involve determining energy savings for a case study building and the inclusion of additional experimental data to refine the annual savings values. Further comparisons to non-published energy savings values and efficiencies will be made.

References

[1] Hall R, Design Guidance on Transpired Solar Collectors in Renovation, Renovation of Buildings using Steel Technologies (ROBUST), 2011 WP 1.8.
[2] Allwinkle, S. The Chartered Institute of Architectural Technologists ISSN 1361-326X (2011) Issue 95
[3] Soteris A. Kalogirou, Solar thermal collectors and applications Progress in Energy and Combustion Science. 30 (2004) 231–295
[4] Hollick, J. C. Unglazed solar wall air heaters. Renewable Energy, (1994) 5, 415-421
[5] BS EN 12975-2:2006 "thermal solar systems and components, solar collectors"
[6] BS EN 308:1997 " Heat exchangers-Test procedures for establishing the performance of air to air flue gases heat recovery devices
[7] BS 848-1:1997 "Fans for general purposes. Performance testing using standardized airways"
[8] ISO 5801: 1997 "Industrial fans: Performance testing using standardized airways"
[9] CBSE guide C: 2007, ISBN 0 7506 5360 4
[10] A.L. Buck. "New equations for computing vapour, pressure and enhancement factor "Journal of applied meteorology, Vol. 20 nº 12 (1981), pp 1527-1532